Experimental evidence of power-law trapping-time distributions in porous media

German Drazer*
Grupo de Medios Porosos, Facultad de Ingeniería, Universidad de Buenos Aires, Paseo Colón 850, 1063 Capital Federal, Argentina

Damián H. Zanette
Consejo Nacional de Investigaciones Científicas y Técnicas, Centro Atómico Bariloche and Instituto Balseiro, 8400 San Carlos de Bariloche, Argentina

(Received 17 March 1999)

We present experimental results of solute transport in porous samples made of packings of activated carbon porous grains. Exchange experiments, where the tagged solution initially saturating the medium is replaced with the same solution without tracer, are accurately described by macroscopic transport equations. On the other hand, in desorption experiments, where the tagged solution is replaced by water, the solute concentration exhibits a power-law decay for long times, which requires a more detailed, mesoscopic description. We reproduce this behavior within a continuous-time random-walk approach, where the waiting time distribution is related to the desorption isotherm. Results are compatible with a power-law trapping time distribution with divergent first moment, characteristic of anomalous (sub)diffusion. [S1063-651X(99)14411-8]

PACS number(s): 47.55.Mh, 05.40.−a

I. INTRODUCTION

Transport processes in porous media are a widespread phenomenon in nature as well as in many applications [1]. Besides having considerable practical interest, this kind of process is a paradigm of anomalous diffusion, which has attracted much attention in the last decade [2]. In anomalous diffusive transport the proportionality between the mean square displacement of a particle, $\langle x^2 \rangle$, and the time t breaks down, and is often replaced by a relation of the type $\langle x^2 \rangle \propto t^{\beta}$ with $\beta \neq 1$. The case of $\beta < 1$, usually referred to as subdiffusion is characteristic of transport in porous media.

Much analytical work has been devoted to study anomalous diffusion at different levels of description [2], especially, within mesoscopic, random-walk models. In particular, subdiffusion has been modeled assigning a power-law waiting time with divergent mean value to a continuous-time random walk (CTRW) [3]. This approach has made it clear that a connection exists between anomalous properties of the transport process and strong inhomogeneities in the underlying medium. However, such models involve often very simplified assumptions on the physical structure of the medium. In this respect, comparison of the analytical predictions with experimental results becomes crucial.

The purpose of the present paper is to report experimental results of transport in porous samples made of packings of activated carbon porous grains [4]. Two different kinds of tracer-dispersion experiments were carried out. In the first one, a tagged solution which initially saturates the medium is displaced by the same solution but without tracer (exchange experiments). In the second, water displaces the tagged solution (desorption experiments). In exchange experiments the total solute concentration remains constant. In this case, where the number of adsorbed particles is a fixed fraction of the total number of solute particles, the local evolution of concentrations can be accurately described by means of macroscopic transport equations. Such equations have been widely applied to problems involving porous media in many fields, such as oil exploitation [5,6], chemical engineering [7], soil science [8], and fluid dynamics [9].

On the other hand, in desorption experiments the total concentration vanishes with time. More specifically, experiments show that the long-time behavior of tracer concentration exhibits power-law tails. A relevant question is how these tails are related to the microscopic features of transport inside the carbon grains and, in particular, to the trapping times of tracer particles. In contrast to the case of exchange experiments, the macroscopic approach fails here to correctly explain the time dependence of concentrations.

To address the above question we follow thus a statistical mechanical approach at the mesoscopic level. We start considering the adsorption isotherm, which relates, at a fixed temperature, the concentration of adsorbed particles to the concentration of particles in solution. The adsorption isotherm can be experimentally determined [10] and, for certain limits in the concentration domain, admits to be phenomenologically represented by simple analytical expressions. We find then a connection between this isotherm and the trapping-time distribution associated with the adsorption sites in the medium. Finally, we associate such a distribution with the waiting-time distribution of a CTRW in a one-dimensional model of the porous medium. Within this frame, we are able to derive the long-time behavior of the total solute concentration in the desorption process, taking into account the low-concentration limit of the desorption isotherm. Nonlinearities in this isotherm, whose effects have been scarcely studied in previous work [11], are crucial in defining the form of the concentration decay. Our results, which are in reasonable agreement with experiments, suggest that assigning a power-law trapping-time distribution to the adsorption sites in the activated carbon porous medium is a realistic assumption.

*Electronic address:gdrazer@tron.fi.uba.ar

II. EXPERIMENT

A. Sample characterization

Porous samples used in the experiments are nonconsolidated packings of relatively uniform, spherical, activated carbon grains obtained from apricot pit. The mean diameter of the carbon grains is $d=(0.13\pm0.01)$ cm. The carbon grains were packed in a 30 cm length, 2.54 cm inner-diameter cylinder (cross section $A=5.1$ cm^2). The packing procedure, intended to obtain homogeneous samples, is described elsewhere [12,13].

Porosity is defined as the ratio of the volume accessible to an intruding fluid to the total volume of the medium. Our samples have two classes of pores; i.e., they constitute a double-porosity medium [1]. We therefore distinguish between internal and external porosities. The internal porosity is associated with the accessible volume inside the carbon grains. Its mean value $\Phi_i=0.45\pm0.05$ has been measured by spontaneous imbibition of distillated water. The pore size distribution (PSD) was independently determined by nitrogen adsorption and mercury intrusion, and ranges approximately from near-atomic scales up to 10^{-4} cm [10]. The total cumulative porosity obtained from the PSD, $\Phi_{\mathrm{PSD}}=0.49$, is consistent with the effective porosity Φ_i seen by tracer particles.

The external (packing) porosity of the samples is associated with the accessible volume outside grains. Its value $\Phi_e=0.45\pm0.02$ has been determined by comparing the total volume to the volume of the carbon grains, considering the carbon grains as nonporous solids. The total porosity of the samples Φ is readily obtained from the internal and external porosities,

$$\Phi=\Phi_e+(1-\Phi_e)\Phi_i=0.70\pm0.06. \tag{1}$$

The adsorption properties of the samples at a given temperature are characterized by the adsorption isotherm. This isotherm relates the total concentrations of solute in solution C_T and of adsorbed solute S_T. A phenomenological approach to the analytical form of this relation is the Freundlich adsorption isotherm, which assumes an algebraic dependence of S_T on C_T. In a previous experiment [10], the Freundlich isotherm for the carbon grains imbibited by NaI aqueous solution was found:

$$S_T=kC_T^{\mu}, \tag{2}$$

with $k=1.0\pm0.4$ and $\mu=0.63\pm0.13$. Here, C_T and S_T are molar concentrations.

Plastic grids were placed at both ends of the samples, preventing outflow of the carbon grains. A few layers of glass beads placed at the inlet insure a radially uniform injection of fluid over the whole cross section of the porous medium [14].

B. Dispersion measurements

In the experiments, the porous medium is initially filled with aqueous 0.1 M NaI solution tagged with I^{131}. In the saturation procedure and during the experiments, the medium is placed vertically in order to avoid flow inhomogeneities across the sample section due to gravity-induced segregation. Interfaces are stable when the more dense fluid displaces the less dense one.

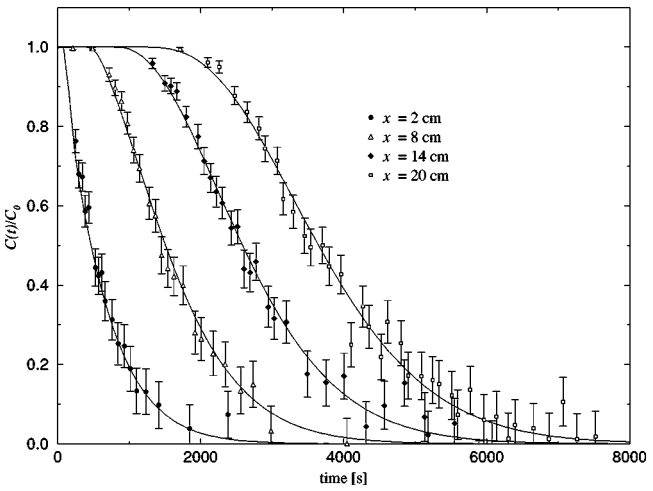

FIG. 1. Time dependence of the tracer concentration recorded at four different positions x along the sample in an exchange experiment. The dots correspond to the experimental data. Solid lines correspond to the best fit with solutions of Eqs. (7) [$f=0.65\pm0.02$, $\mathcal{R}=1.4\pm0.3$, $v=8.2\times10^{-3}$ cm/s, $D=(1.1\pm0.5)\times10^{-3}$ cm^2/s, $D_s=(1.9\pm0.7)\times10^{-6}$ cm^2/s].

We performed measurements of tracer desorption and dispersion, in which a stepwise variation in the concentration of I^{131} is induced at time $t=0$ and kept constant thereafter. The displacing fluid is injected at a constant flow rate. The effluent, collected over a computer controlled electronic scales, allows one to measure and control the injection rate. The radioactive tagging technique makes it possible to record tracer concentration variations at different cross sections of the porous medium, through activity measurements. Gamma radiation from tracer particles inside the porous sample is collimated by a lead block with a 0.3 cm slot, through which radiation activity is measured by a standard scintillation detector.

As advanced in the Introduction, experiments are carried out with two different displacing fluids, namely, an untagged NaI solution at the same concentration as the tagged solution (exchange experiments) and distillate water (desorption experiments).

C. Results

The dots in Fig. 1 stand for measurements of the tracer concentration $C(t)$ as a function of time, normalized to the initial concentration, in an exchange experiment. Different symbols correspond to measurements at different distances from the inlet, as indicated in the caption. On the average, as the untagged solution replaces the tagged one, $C(t)$ decreases steadily approaching zero for large times.

Figure 2 shows measurements of tracer concentration in a desorption experiment. The tagged solution is now being replaced by water and the solute is being eliminated from the medium, so that $C(t)$ approaches zero again. However, it is apparent from comparison with Fig. 1 that the concentration decay exhibits longer tails for large times. The same data are shown in Fig. 3 in a log-log plot. It is clear that those tails

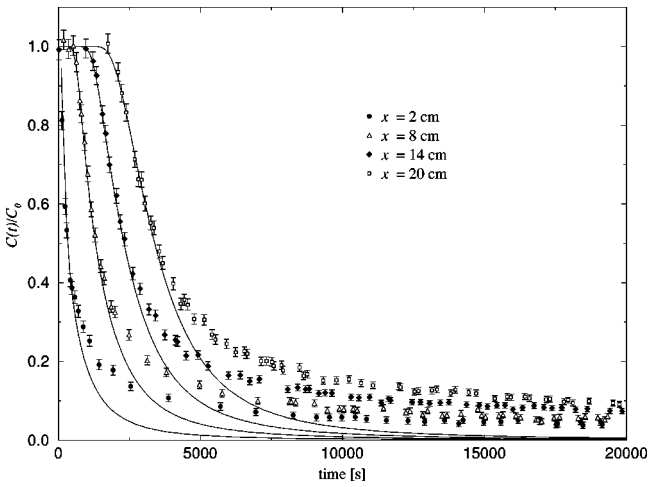

FIG. 2. Time variation of tracer concentration in a desorption experiment. Dots correspond to experimental data recorded at four different positions x along the sample, with $v=8.8\times10^{-3}$ cm/s. Solid lines corresponds to numerical solutions of Eqs. (9), where the parameters $f=0.65$, $D=1.1\times10^{-3}$ cm^2/s and $D_s=(1.9\pm0.7)\times10^{-6}$ cm^2/s were computed from exchange experiments. The isotherm parameters used are $k=0.65\pm0.05$ and $\mu=0.65\pm0.05$ in agreement with the result $\mathcal{R}=1.4\pm0.3$ of exchange experiments.

follow a power law with the same exponent $\mu=0.63$ for each data set.

In Fig. 4, we show measurements taken at a fixed distance from the inlet for different flow velocities in desorption experiments. The power-law exponent is again the same for the three data sets.

Errors bars, displayed in all the figures, correspond to the uncertainty in the activity measured by the scintillation detector.

III. MACROSCOPIC APPROACH

In order to explain our experimental results, we apply first a macroscopic formulation based on transport equations for the relevant concentrations. As advanced before, the porous

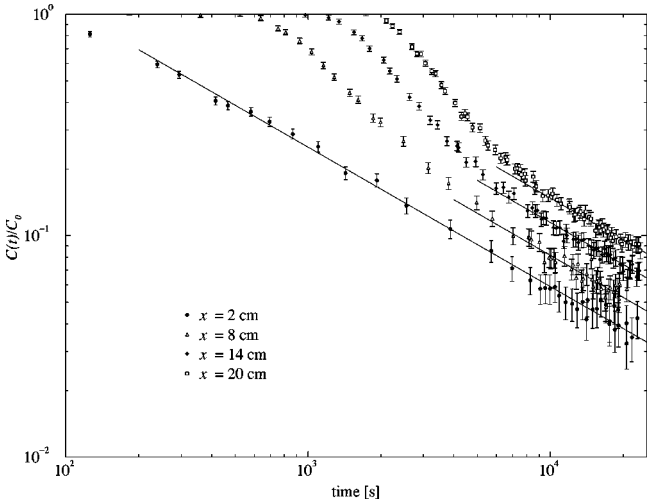

FIG. 3. Time variation of tracer concentration in a log-log plot. The experimental data corresponds to the desorption experiment shown in Fig. 2. Straight lines correspond to the long-time behavior predicted in Eq. (22), whose exponent corresponds to that of the adsorption isotherm, $\mu=0.63$.

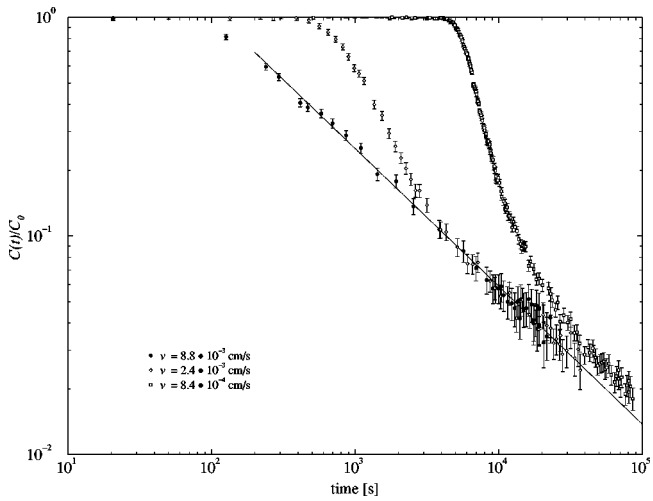

FIG. 4. Time variation of tracer concentration in desorption experiments with different flow velocities v, at $x\approx2$ cm from the inlet. The straight line corresponds to the predicted power-law tail at long times, whose exponent corresponds to that of the adsorption isotherm $\mu=0.63$.

sample has two different classes of pores. Large pores correspond to voids in the packing structure, and compose the external transport paths. Small pores are found inside the carbon grains, and determine internal transport paths. The permeability contrast between these transport paths is very high, with a permeability ratio of about 10^6 [15]. It can be shown that, due to this large permeability contrast, in the range of injection rates investigated convection is dominant outside the grains while diffusion is the only relevant transport mechanism in the internal paths. Therefore, the volume of internal pores may be considered as a stagnant zone, where tracer particles get trapped and convective transport is negligible.

Assuming that a fraction $1-f$ of the total volume of pores is occupied by stagnant zones, we can employ the following set of transport equations [16]:

$$f\frac{\partial C_m}{\partial t}+(1-f)\left(\frac{\partial\langle C_i\rangle}{\partial t}+\frac{\partial\langle S_i\rangle}{\partial t}\right)=D\frac{\partial^2 C_m}{\partial x^2}-v\frac{\partial C_m}{\partial x}, \tag{3a}$$

$$\frac{\partial C_i}{\partial t}+\frac{\partial S_i}{\partial t}=D_s\left(\frac{\partial^2 C_i}{\partial r^2}+\frac{2}{r}\frac{\partial C_i}{\partial r}\right). \tag{3b}$$

Here, $S_i(r,x,t)$ is the adsorbed solute concentration inside the grains, whereas $C_m(x,t)$ and $C_i(r,x,t)$ correspond to the solute concentration in mobile and stagnant zones, respectively. The diffusivities in these zones are D and D_s, and v stands for the flow velocity, which is imposed at the inlet. The coordinate x is measured along the sample from the inlet, and r is the radial coordinate inside the spherical carbon grains. The mean values $\langle\cdot\rangle$ stand for volume averages inside the grains. The first equation relates the evolution of solute concentration in mobile fluid zones, the volume-averaged solute concentration inside the grains, the longitudinal dispersion, and the convective transport. The second equation stands for the evolution of the solute concentration inside the grains, due to diffusive transport. The initial and boundary conditions corresponding to our experiments are, respectively,

$$C_m(x,0)=C_0, \quad x>0, \tag{4a}$$

$$C_i(r,x,0)=C_0, \quad x,r>0, \tag{4b}$$

and

$$C_m(0,t)=0, \quad t>0, \tag{5a}$$

$$C_m(x,t)=C_i(r=a,x,t), \quad x,t>0, \tag{5b}$$

where $a=d/2$ is the grain radius. The boundary condition at the grain surface, Eq. (5b), couples Eqs. (3a) and (3b).

Assuming that the adsorption process is at equilibrium and, using Eq. (2), solutions to Eqs. (3) can be numerically obtained by means of standard finite-difference schemes [17,18]. Both exchange and desorption situations can be considered. However, as advanced in the Introduction, the nature of such solutions and their accuracy in reproducing experimental results depends strongly on which kind of experiment is being described.

A. Exchange experiments

In this case, both the total adsorbed concentration S_T and the total concentration in solution, C_T, remain constant. Therefore, activity measurements are sensible to variations of tracer concentration inside the sample. We will thus use Eq. (3) to describe these variations at different cross sections of the porous medium.

Due to the fact that the total concentration is kept constant, the adsorption equilibrium is undisturbed during the experiments, and the resulting adsorption isotherm for tracer particles is linear:

$$S_i=\frac{S_T}{C_T}C_i=kC_T^{\mu-1}C_i=\mathcal{R}(C_T)C_i, \tag{6}$$

where we have taken into account that the proportion of adsorbed tagged particles, S_i/S_T, should be equal, at equilibrium, to the fraction of tagged particles in solution, C_i/C_T.

Assuming that the adsorption process is enslaved to diffusion, namely, that the concentration of adsorbed tagged particles follows instantaneously the local variations of tracer concentration in the solution, and using Eq. (6), we can rewrite Eqs. (3) as follows:

$$f\frac{\partial C_m}{\partial t}+(1-f)(1+\mathcal{R})\frac{\partial\langle C_i\rangle}{\partial t}=D\frac{\partial^2 C_m}{\partial x^2}-v\frac{\partial C_m}{\partial x}, \tag{7a}$$

$$\frac{\partial C_i}{\partial t}=\frac{D_s}{1+\mathcal{R}}\left(\frac{\partial^2 C_i}{\partial r^2}+\frac{2}{r}\frac{\partial C_i}{\partial r}\right). \tag{7b}$$

Solutions to Eqs. (7) accurately fit experimental results obtained at different cross sections along the porous medium, as shown in Fig. 1. Let us emphasize that the whole of experimental data have been fitted by numerical results with a single set of parameters. These parameters are in good agreement with previous experiments $[D_s=(1.5\pm0.1)\times10^{-6}$ cm^2/s, $D\sim dv$ [10,15]] and with model assumptions $[f=\Phi_i/\Phi_T=0.65\pm0.08, \quad \mathcal{R}(C_T)=kC_T^{\mu-1}=2.3\pm1.5]$. A detailed study of the parameter dependence on the injection rate can also be found in previous publications [12,15].

B. Desorption experiments

In desorption experiments the total concentration varies with time. The concentration of tagged particles is now directly proportional to that of the solute. Therefore, activity measurements can be used to determine variations in the total solute concentration. Total concentrations inside and outside the grains will be denoted in the following discussion by C_m (total solute concentration in solution inside the external paths), C_i (total concentration solution inside the internal paths), and S_i (total adsorbed solute concentration inside the grains).

Let us assume, as before, that the adsorption process is fast enough to be considered as locally enslaved to diffusion. The adsorbed solute concentration S_i is thus related to the local concentration in solution C_i by the adsorption isotherm [Eq. (2)], and therefore

$$\frac{\partial S_i}{\partial t}=k\frac{\partial C_i^{\mu}}{\partial t}. \tag{8}$$

Using this relation and rewriting Eqs. (3) for the total solute concentration, we obtain

$$f\frac{\partial C_m}{\partial t}+(1-f)\frac{\partial}{\partial t}\langle C_i+kC_i^{\mu}\rangle=D\frac{\partial^2 C_m}{\partial x^2}-v\frac{\partial C_m}{\partial x}, \tag{9a}$$

$$\frac{\partial}{\partial t}(C_i+kC_i^{\mu})=D_s\left(\frac{\partial^2 C_i}{\partial r^2}+\frac{2}{r}\frac{\partial C_i}{\partial r}\right). \tag{9b}$$

Even though the initial part of the desorption process can be accurately described by the numerical solutions to these equations, the anomalously long tails of experimental curves can no longer be fitted, as shown in Fig. 2. Numerical results predict in fact systematically lower concentrations for large times.

Since the macroscopic transport equations are not able to describe the evolution of desorption experiments at large times, i.e., at low concentrations, we will formulate an analytical description at a mesoscopic level. More specifically, we will attempt to predict the observed algebraic tails in terms of a one-dimensional continuous time random walk model [19]. This requires us to relate first the CTRW waiting-time distribution, to be associated with the trapping times inside the carbon grains, to the Freundlich adsorption isotherm.

IV. MESOSCOPIC APPROACH

A. Statistical approach to the Freundlich isotherm

It is a well known fact that the Freundlich adsorption isotherm describes with very good accuracy experimental data. Since its empirical formulation, several authors have provided derivations within statistical mechanical approaches, considering inhomogeneous adsorption surfaces [20–24]. In these derivations, the surface is characterized by a probability distribution for the adsorption-site energies. Single occupancy of adsorption sites (monolayer coverage) and no lateral interaction between adsorbed particles (noncooperative adsorption) are assumed [24]. Moreover, the number of adsorption sites is fixed.

We will follow this approach closely but, instead of defining a distribution of energies over the surface sites, we

introduce a distribution of trapping times. The trapping time τ is defined as the time spent inside the grains by an adsorbed particle. Assuming single occupancy, the Langmuir adsorption equation [25] applies for each value of τ,

$$\theta(\tau)=\frac{wC_i\tau}{1+wC_i\tau}, \tag{10}$$

where $\theta(\tau)$ is the Langmuir coverage [4]. The constant w is inversely proportional to the mean time τ_l spent by solute particles in the liquid phase and to the molar concentration of adsorption sites S_s, namely, $w=(\tau_l S_s)^{-1}$. Let us note that S_s equals the saturation concentration.

If $\varphi(\tau)d\tau$ is the fraction of sites whose characteristic trapping time lies between τ and $\tau+d\tau$, Eq. (10) implies that the overall adsorbed concentration is given by

$$S_i=S_s\int_0^\infty \frac{wC_i\tau}{1+wC_i\tau}\varphi(\tau)d\tau. \tag{11}$$

Taking into account Eq. (2), Eq. (11) makes it possible to evaluate the trapping-time probability density function (PDF) $\varphi(\tau)$. Combining both equations, in fact, we get

$$kC_i^\mu=S_s\frac{1}{C_i}\int_0^\infty \frac{wx}{1+wx}\varphi(x/C_i)dx, \tag{12}$$

where we have replaced $C_i\tau$ by x. This equation relates the limit of low solute concentration ($C_i\sim 0$) to the behavior of $\varphi(\tau)$ for large trapping times. On the other hand, if the Freundlich isotherm is assumed to hold in the limit of high solute concentrations ($C_i\to\infty$), according to which the adsorbed concentration increases without bound, the resulting PDF is non-normalizable [23]. This result is a direct consequence of the assumptions of fixed number of adsorption sites and monolayer coverage. Several possible modifications to the adsorption isotherm, which reduce to the Freundlich expression when C_i is small, have been proposed [4,23,21,22]. Nevertheless, since we are interested in describing the behavior at small solute concentrations, we use the Freundlich isotherm without taking into account possible corrections at high concentrations. The range where the concentration varies in desorption experiments ($C_i\lesssim 0.1$ M) is in fact within the experimental range where the adsorption isotherm was previously determined. Thus, as the Freundlich isotherm is a reasonably good empirical description of our experimental data, the large-τ asymptotic behavior of the trapping-time PDF should be correctly determined using Eq. (11).

Let us then discuss the limit of low solute concentrations. Using straightforward scaling arguments, Eq. (12) implies that the trapping-time PDF has a power-law behavior for long times,

$$\varphi(\tau)\sim T^\mu/\tau^{1+\mu}, \tag{13}$$

where T is a constant with dimensions of time. More rigorously, treating Eq. (12) as an integral equation where the left hand side is known, and applying standard results [note that Eq. (12) can be related to a Stieltjes transform, as first pointed out by Sips [23]], it can be shown that $\varphi(\tau)\propto\tau^{-(1+\mu)}$ over the whole range of trapping times $\tau\in(0,\infty)$. This gives, as already mentioned, a non-normalizable PDF, due to the high-concentration behavior of the Freundlich isotherm.

Finally, let us note that the asymptotic behavior of $\varphi(\tau)$ implies a divergent mean trapping time, as the exponent lies in the range $0<\mu<1$,

$$\langle\tau\rangle=\int_0^\infty \tau\varphi(\tau)d\tau=\infty. \tag{14}$$

In fact, it can be shown from Eq. (11) that a distribution with mean trapping time leads to a linear regime, $S_i\sim(\langle\tau\rangle/\tau_l)C_i$, at sufficiently low solute concentrations (Henry's law [4]).

B. Continuous-time random walk approach

In this section we will describe tracer transport in our porous samples by means of a continuous-time random walk [26,19,2]. The medium is represented as a one-dimensional N-site lattice along which each tracer particle is convected. At each site the tracer particle gets trapped during a time τ before a new convective step is performed in the direction of the flow. Trapping times are distributed according $\varphi(\tau)$.

In this decoupled CTRW model the distance ξ between successive traps is given by the mean length of a convective path performed entirely in the external channels, i.e., without visiting the internal paths. On the other hand, the long-time behavior of the trapping-time PDF will be dominated by adsorption effects in the internal paths and is given by Eq. (13). This approach is valid at low solute concentrations, when the interaction between solute particles can be neglected. We show in the following that this very simple model makes it possible to predict the power-law tail observed in desorption experiments, which is thus to be associated with the long-time tail of the trapping-time PDF.

We aim at calculating the probability distribution $P(x,t)$ for a tracer particle to be at site x at time t, assuming that it was at $x=0$ at $t=0$. Following Montroll and Weiss [19], let $Q(x,t)$ be the PDF for the tracer particle to reach x at time t, and let $\Psi(t)$ be the probability that the elapsed time between successive convective steps is at least t, i.e.,

$$\Psi(t)=1-\int_0^t\varphi(\tau)d\tau. \tag{15}$$

Then

$$P(x,t)=\int_0^t Q(x,\tau)\Psi(t-\tau)d\tau. \tag{16}$$

Since the particles are convected the same length ξ at each jump, $Q(x,t)$ equals the probability $P_n(t)$ that a tracer particle has performed $n=x/\xi$ jumps exactly at time t [27], whence, in the Laplace domain, it follows that

$$\begin{aligned}P(x,u)&=\Psi(u)Q(x,u)\\&=\Psi(u)P_n(u)=\Psi(u)[\varphi(u)]^n=\frac{1-\varphi(u)}{u}[\varphi(u)]^n.\end{aligned} \tag{17}$$

Taking into account that convective steps occur in the flow direction only, the normalized initial condition for $P(x,t)$ in desorption experiments corresponds, in this lattice model, to

$$P(j\xi,t=0)=\frac{1}{N}, \quad 0<j\leqslant N=x/\xi. \tag{18}$$

Thus, the probability for the tracer particle to be at x at time t is, in the Laplace domain,

$$P(x,u)=\frac{1}{N}\Psi(u)\sum_{n=0}^{N-1}[\varphi(u)]^n=\frac{1-[\varphi(u)]^N}{Nu}. \tag{19}$$

Finally, to find the large-time behavior of $P(x,t)$ it is necessary to use the asymptotic form of $\varphi(u)$ in the neighborhood of $u=0$. For the power-law tail given in Eq. (13) this asymptotic form is [28]

$$\varphi(u)\sim 1-(uT)^{\mu}. \tag{20}$$

With this expansion we can compute the small-u limit for $P(x,t)$:

$$P(x,u)\sim T^{\mu}u^{\mu-1}. \tag{21}$$

Thus, via a Tauberian theorem for Laplace transforms [28], we infer that

$$P(x,t)\sim\left(\frac{T}{t}\right)^{\mu}. \tag{22}$$

This is our final result, which predicts that power-law tails observed in desorption experiments should have the same exponent μ as the adsorption isotherm, at any distance x from the inlet section and at any injection rate. The slope of straight lines in the log-log plots of Figs. 3 and 4 is -0.63, which corresponds to the value of the exponent μ in the Freundlich isotherm (2). The agreement with the power-law decay observed in desorption experiments is reasonably good.

V. SUMMARY AND DISCUSSION

We have presented results of exchange and desorption experiments in activated carbon porous media. In exchange experiments the total solute concentration remains constant while a stepwise variation in the tracer concentration is induced at the inlet. In this case we have shown that a macroscopic description, in terms of transport equations for the relevant concentrations, provides an accurate description of variations in the tracer concentration at different cross sections of the porous medium. Moreover, the macroscopic parameters and their dependence on injection rate can be related to the porous medium physicochemical properties, namely, the internal and external porosities, the adsorption isotherm, the diffusion coefficient inside the grains, and the carbon grain size [15]. On the other hand, even though the macroscopic description agrees with experimental data in the initial part of the desorption process, the long-time behavior exhibited by desorption curves differs considerably from the analytical macroscopic approach. In particular, the power-law time dependence of the solute concentration is not reproduced by the solutions to the macroscopic equations.

This anomalous behavior could be accounted for by introducing a continuous-time random walk model for the desorption-dispersion process. The long-time behavior of the trapping-time distribution was derived from a microscopic model which correctly describes the limit of low concentrations in the experimentally measured adsorption isotherm. The microscopic model of the adsorbing surface is a variation of previous models [23,21], but avoids a description of adsorption sites in terms of bonding energies. Therefore, it makes it possible to include geometric effects in the distribution of trapping times inside the carbon grains. Within this model, we were able to infer, from the Freundlich isotherm, a distribution for trapping times in the porous medium. In particular, we have found that this distribution has a power-law tail with the same exponent as the isotherm, which in turn implies a power-law decay in the tracer concentration observed in the experiments. Moreover, the predicted power-law long-time behavior does not depend on the distance from the inlet or on the injection rate, as is also observed in the experiments.

A relevant question regards the possible existence of a critical concentration at which this anomalous behavior appears. More specifically, we expect that the power-law decay of the solute concentration appears when a critical relation between this concentration, the distance x from the inlet, and the convective step length ξ is satisfied. Establishing this relation will be the object of future experimental and theoretical work. Furthermore, in order to study the observed anomalous behavior in detail, it would be interesting to carry out desorption experiments where the initial solute concentration is low enough for the solute particles to be considered as noninteracting throughout the experiment. In this case, recording the time evolution of the dispersion front and of the average solute distance from the inlet would be a suitable tool to test the theoretical predictions of our model. Namely, the anomalous broadening of the mixing zone, given by the mean-square displacement for a single particle, should grow as $t^{2\mu}$, while the average distance from the inlet should increase as t^{μ}.

ACKNOWLEDGMENTS

D.H.Z. acknowledges financial support from Fundación Antorchas, Argentina. G.D. thanks J. Busch for fruitful discussions. G.D. has been supported by CONICET Argentina.

[1] J. P. Hulin, Adv. Colloid Interface Sci. **49**, 47 (1994).

[2] J. P. Bouchaud and A. Georges, Phys. Rep. **195**, 127 (1990), and references therein.

[3] See, for instance, J. Klafter, G. Zumofen, and M. F. Shlesinger, in *Lévy Flights and Related Topics in Physics*, edited by M. F. Shlesinger, G. M. Zaslavski, and U. Frisch (Springer, Berlin, 1995).

[4] D. M. Ruthven, *Principles of Adsorption and Adsorption Processes* (Wiley, New York, 1984).

[5] K. H. Coats and B. D. Smith, Soc. Pet. Eng. J. **231**, 73 (1964).

[6] K. S. Sorbie, A. Parker, and P. J. Clifford, SPE Reservoir Eng. **2** (3), 281 (1987).
[7] A. Rasmuson and I. Neretnieks, AIChE. J. **26**, 686 (1980).
[8] J. P. Gaudet, H. Jégat, G. Vachaud, and P. J. Wierenga, Soil Sci. Soc. Am. J. **41**, 665 (1977).
[9] E. Charlaix, J. P. Hulin, and T. J. Plona, Phys. Fluids **30**, 1690 (1987).
[10] G. Drazer, R. Chertcoff, L. Bruno, and M. Rosen, Chem. Eng. Sci. **54**, 4285 (1999).
[11] C. N. Dawson, C. J. V. Duijn, and R. E. Grundy, SIAM (Soc. Ind. Appl. Math.) J. Appl. Math. **56**, 965 (1996).
[12] G. Drazer, R. Chertcoff, L. Bruno, and M. Rosen, in *Fundamentals of Adsorption VI*, edited by F. Meunier (Elsevier, Paris, 1998), pp. 727–732.
[13] P. Magnico *et al.*, Phys. Fluids A **5**, 46 (1993).
[14] C. Grattoni, M. Rosen, R. Chertcoff, and S. Bidner, Chem. Eng. Sci. **42**, 47 (1987).
[15] G. Drazer, R. Chertcoff, L. Bruno, M. Rosen, and J. P. Hulin, Chem. Eng. Sci. **54**, 4137 (1999).
[16] For a review, see M. Sahimi, Rev. Mod. Phys. **65**, 1393 (1993).
[17] J. Crank, *The Mathematics of Diffusion* (Oxford University Press, London, 1956).
[18] H. Press, W. T. Vetterling, S. A. Teukolsky, and B. P. Flannery, *Numerical Recipes in C: The Art of Scientific Computing*, 2nd ed. (Cambridge University Press, Cambridge, England, 1988).
[19] E. W. Montroll and G. H. Weiss, J. Math. Phys. **6**, 167 (1965).
[20] G. Halsey and H. S. Taylor, J. Chem. Phys. **15**, 624 (1947).
[21] R. Sips, J. Chem. Phys. **18**, 1024 (1950).
[22] M. S. da Rocha *et al.*, J. Colloid Interface Sci. **185**, 493 (1997).
[23] R. Sips, J. Chem. Phys. **16**, 490 (1948).
[24] J. M. Honig and E. L. Hill, J. Chem. Phys. **22**, 851 (1954).
[25] R. Kubo, *Statistical Mechanics* (North-Holland, Amsterdam, 1988).
[26] E. W. Montroll, Proc. Symp. Appl. Math. Am. Math. Soc. **16**, 193 (1964).
[27] A. Compte, R. Metzler, and J. Camacho, Phys. Rev. E **56**, 1445 (1997).
[28] W. Feller, *An Introduction to Probability Theory and Its Applications* (Wiley, New York, 1971), Vol. 2.